The fate of the elastic string: roughening near the depinning threshold

1995 J. Phys. A: Math. Gen. 28 1861

(http://iopscience.iop.org/0305-4470/28/7/010)

J. Phys. A: Math. Gen. 28 (1995) 1861–1877. Printed in the UK

The fate of the elastic string: roughening near the depinning threshold

Henrik Jeldtoft Jensen

Department of Mathematics, Imperial College, 180 Queen's Gate, London SW7 2BZ, UK

Received 4 November 1994, in final form 6 February 1995

Abstract. Simulations of an elastic string in $1+1$ dimensions near and at the depinning threshold f_c are presented. The spatial dependence of the roughness is characterized by two exponents. One, $\eta \simeq 0.9$, describes the height–height correlations. The other, $\chi \simeq 1.15$, measures how the transverse width, W, of the string increases with increasing string length. Since $\chi > 1$ any physical string will eventually break as its length is increased. The growth of the width of the string with time is controlled by an exponent $\beta \simeq 0.9$. As the applied driving force approaches f_c from above the width increases according to $W \sim (f - f_c)^{-\sigma}$ with $\sigma \simeq 3$. The dependence of f_c on the strength of the random potential is found to be in agreement with the collective pinning theory by Larkin and Ovchinnikov.

1. Introduction

The present paper is concerned with the motion of an elastic string through a static random potential (*not random forces*). A model with continuous variables is simulated using overdamped dynamics. We concentrate, in particular, on the behaviour precisely at, and in the immediate vicinity above, the depinning threshold. We study the threshold force, the distribution of energy discontinuities, the roughness exponents and the relation between the applied force and the resulting velocity.

The motion of an elastic medium through a static random potential is a model of a variety of physical phenomena. Whenever we drag our spoon out of our cup of tea we observe the interaction of the elastic triple line with the uneven surface of the teaspoon [1, 2] The triple line is the line were the liquid, the air, and the solid all meet. Other examples include the motion of flux lines through the pinning potential of superconductors [3], the motion of charge density waves [4] and surface growth in a dirty environment [5].

The simplest version of this type of physics is a one-dimensional string moving through a two-dimensional background of random pinning centres [6–10]. This model should be directly connected to the triple line pinning, and also to flux lines as well as surface growth in restricted geometries.

The behaviour of such systems is characterized by the existence of a non-zero friction or pinning force which has to be overcome in order to make the elastic line move. One would like to be able to calculate this threshold force from the properties of the random potential together with the elastic properties of the string. The most celebrated attempt at such a calculation is the Larkin–Ovchinnikov (LO) collective pinning theory [11]. In this approach the pinning force is estimated from the fluctuations in the random forces within regions of the elastic medium which are only slightly distorted. In the following we will compare

0305-4470/95/071861+17$19.50

the Larkin–Ovchinnikov estimate with our numerical simulations. We do find agreement with the observed dependence on the amplitude of the random pinning potential. The same agreement was not encountered in two-dimensional model simulations [12]. In this paper we will discuss an alternative derivation of the threshold force [13]. This method focuses on the connection between the threshold force and the discontinuities in the potential energy of the system caused by elastic instabilities.

As the string is moved through the random potential, either at threshold or just above threshold, it becomes rough. The presence of the static random potential gives rise to roughness exponents which are significantly larger than the Karda–Parisi–Zhang [14,5] (KPZ) values and closer to experimentally observed values [15]. This fact has inspired Parisi [5] to suggest that static disorder is responsible for the discrepancy between the roughness exponent observed experimentally for growing interfaces and the KPZ exponents. We shall, in fact, see that the string studied in the present paper becomes so rough, when the applied driving force is lowered towards the threshold value from above, that the string inevitably breaks [4,7,8].

There have been many recent investigations of the roughning of the elastic string or interface as it is forced through a random background potential or random forces. Nattermann *et al* [16] performed a functional renormalization-group calculation on a diffusion equation containing a quenched random *force term*. Our simulations are done for a random potential. Nevertheless, the simulations yield values for the the dynamical exponent z and the velocity exponent θ in qualitative agreement with their results. Namely, $z < 2$, indicating superdiffusive behaviour at the depinning transition, and $\theta < 1$ leading to a negative curvature of the velocity versus driving force curve. Our simulations are characterized by two roughness exponents. One exponent $\eta \simeq 0.9$ describes the spatial behaviour for a given system size, the other one, $\chi \simeq 1.15$, describes the dependence of the roughness on the size of the system. The value of η is in good agreement with the result obtained by Nattermann *et al* extrapolated to one dimension. The dynamical exponent is obtained as $z = \eta/\beta$, where $\beta \sim 0.9$ describes the time evolution of the roughness. The other exponent χ does not appear in their treatment. Narayan and Fisher have suggested that $\eta = 1$ [17]. Our simulation might, in fact, be consistent with $\eta = 1$ in the limit of long strings. The paper by Nattermann *et al* also contains a derivation of an expression for the depinning threshold. Their estimate agrees with the one obtained from collective pinning theory [11]. In section 5 below we show that our simulations agree with the collective pinning expression.

Dong *et al* [6] have simulated a model of an elastic string similar to the one studied in the present paper. However, they restricted their analysis of the roughness of the string to a study of the spatial dependence of the height–height correlation function for fixed system size. For this reason they failed to observe the breaking of the string with increasing system size [7,8].

In connection with modelling of interface growth there has appeared a range of studies of discrete time step cellular automata-like algorithms [5,8–10,18]. These papers are concerned with the increase in the scaling exponents due to static random forces. They include a threshold explicitly in the update algorithm. The work by Roux and Hansen [8] also observes (in agreement with the present paper) that the fluctuations in the interface become so large at long distances that the interface itself is destroyed. The model studied here is similar in spirit to the models studied in these papers [18,5,6,8–10]. It differs in detail by being a continuous dynamics simulation and by including a random potential rather than random forces. Moreover, there is no threshold explicit in our definition of the dynamics of the model. Threshold dynamics arises as a consequence of the continuous equation of motion.

The paper is organized in the following way. In section 2 the details of the model are given and the simulation method is described. In section 3 the behaviour of the string as it is moved at—or in the vicinity above—threshold is presented. We discuss the avalanche activity, the roughness of the string as a function of $f - f_c$, where f is the applied force and f_c is the threshold force. Furthermore, we discuss the velocity–force relation. In section 4 we discuss the breaking of the string. In section 5 we study the scaling of f_c with the amplitude of the random potential. This result is compared with collective pinning theory [11]. We present an alternative definition of the threshold force in terms of the discontinuities in the total energy of the string. Section 6 contains a summary and a discussion of the consequences of the string-breaking to experimental situations.

2. Model

Figure 1 shows a sketch of the system considered in the present paper. A discrete version of an elastic string. The system consist of L beads which can slide on parallel rails. The separation between the rails is equal to one unit of length. The position along the rail of bead number n is denoted by h_n. Pinning centres are positioned at random along the rails. Each of the pinning centres have the same strength. Beads on adjacent rails interact through a harmonic potential. The potential energy of the system is defined by the following equation:

$$V = \tfrac{1}{2}\sum_{n=1}^{N-1}[(h_{n+1} - h_n)^2 + U_p^n(h_n)] \tag{1}$$

where the pinning energy term U_p^n is given by

$$U_p^n(h) = \sum_{z_p^n} U(h - z_p^n) \tag{2}$$

here the sum runs over the positions z_p^n of the pinning centres along the rail number n. All the pinning centres are characterized by the same Gaussian shape of the pinning well:

$$U(s) = -A_p \exp(-(s/R_p)^2)\,. \tag{3}$$

The pinning centres are distributed randomly with the same uniform probability and average density n_p along each rail.

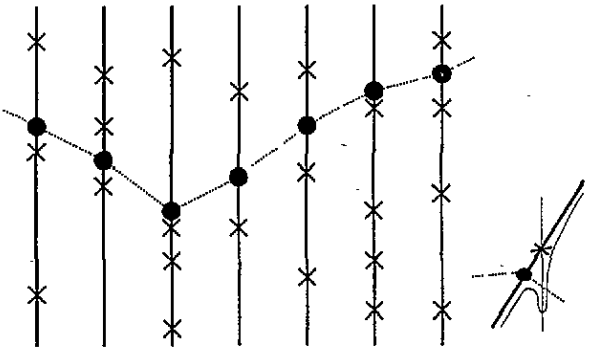

Figure 1. Beads restricted to move along a set of parallel rails. The crosses indicate the random position of Gaussian pinning wells (see the three-dimensional insert to the right of the main figure). The dotted line connecting the beads indicates the elastic coupling.

We are interested in systems which exhibit over-damped dynamics. Hence, we define the equation of motion for the chain by the following set of equations:

$$\eta \frac{\mathrm{d}h_n}{\mathrm{d}t} = f - \frac{\partial V}{\partial h_n} \qquad n = 1, \ldots, L \tag{4}$$

where f is the applied driving force. We fix our time unit by choosing $\eta = 1$.

All simulations start from the straight string. The evolution of the string has three stages (details will be discussed below). A brief initial stage during which the string relaxes to the first pinning centres. Next an intermediate transient stage where the roughness of the string grows monotonically. Finally, the asymptotic long-time regime where the roughness has saturated.

2.1. Simulation method: at threshold

It is very difficult to access the region near or at the threshold for depinning. One problem is caused by slowing-down effects. More and more time steps are needed in order to make the chain move a given distance and hence to maintain a reasonable level of statistical averaging.

Another, and more important problem, comes from the fluctuations in the force produced by the random potential. The applied force f will only be able to move the chain through a certain region of the random background if f at any instance is larger than the total pinning force f_p (per length):

$$f_\mathrm{p} = -\sum_{n=1}^{L} \frac{\partial U_\mathrm{p}^n}{\partial h_n}. \tag{5}$$

The equation of motion (4) averaged over the beads of the chain determines the average velocity $v = \sum_n \dot{h}_n/L$, i.e. the equation of motion for the centre of mass of the chain is

$$v = f + f_\mathrm{p}. \tag{6}$$

Figure 2 shows a sketch of $-f_\mathrm{p}$ as function of the centre of mass (COM) h. The applied force can only move the COM beyond the point h_m if the force can overcome the maximum pinning force, i.e. $f > f_\mathrm{p}(h_m)$. The time average of the COM velocity $\overline{v}$ is, according to (6), given by the broken area on figure 2. This will lead to a discontinuous jump in $\overline{v}$ at $f = -f_\mathrm{p}(h_m)$. We have $\overline{v} = 0$ for $f < -f_\mathrm{p}(h_m)$ and a finite non-zero $\overline{v}$ for $f > -f_\mathrm{p}(h_m)$. This will be the situation as long as f_p exhibits fluctuations as a function of the COM. These fluctuations might vanish in the limit of infinite systems. We shall, however, see below that other problems await us in the large system limit. The first-order nature of the depinning transition was also observed by Kessler *et al* in their simulations of an open chain in a random force field [18].

Thus, it is not possible to drive a finite system right at the threshold by use of (4). We can, however, drive the system in the limit $v \to 0$ by allowing f to vary in time in such a way that the applied force (which is always taken to be spatially homogeneous) at any instance precisely counteracts the force from the random potential at that instance. In this way we make sure that the total force on the string is kept equal to zero. This is how we study the quasi-static motion of the string [12, 19].

The details of the simulation are as follows. The string is moved as a rigid body a small displacement $\mathrm{d}h$ (typically $\mathrm{d}h = 4 \times 10^{-3} R_\mathrm{p}$) by the substitution $h_n \to h_n + \mathrm{d}h$. The COM position changes accordingly from h to $h + \mathrm{d}h$. The string is then allowed to relax to the new environment by use of (4) while the COM is fixed at $h + \mathrm{d}h$. The time step of

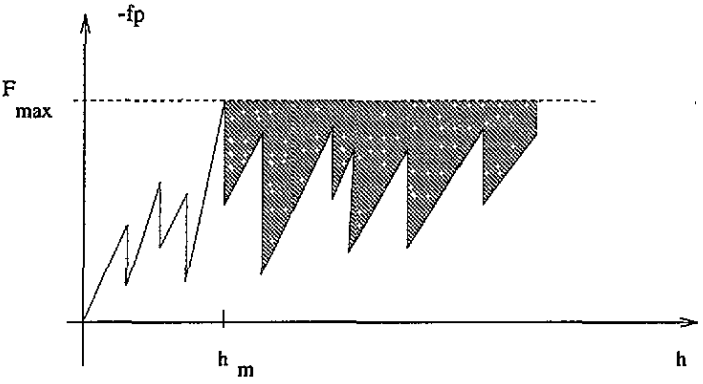

Figure 2. Sketch of the variation of (minus) the total pinning force $-\langle f_p \rangle$ as the centre of mass $\langle h \rangle$ is forced through the pinning potential. The area of the shaded region determines the jump in the centre-of-mass velocity at the depinning threshold.

this annealing is performed in the following way. Equation (4) is used to calculate new positions h_n' of all the beads along the string. The total change in the COM position during this time step is then calculated as $\delta h = \sum(h_n' - h_n)/L$. If $\delta h \neq 0$ we add $-\delta h/L$ to each h_n before we perform the next annealing time step. This is, of course, identical to keeping the total force (pinning forces plus applied forces) on the string exactly equal to zero during the annealing at the COM position $h + \mathrm{d}h$. We typically perform about 40 of these annealing time steps at COM position $h + \mathrm{d}h$ before we once again move the string as a rigid body to the next COM position $h + 2\,\mathrm{d}h$.

2.2. *Simulation method: above threshold*

The simulation of the equation of motion (equation (4)) for an applied spatially homogeneous and time independent force f somewhat larger than the threshold force is straightforward†. We simply discretize (4) directly

$$h_n(t + \Delta t) = h_n(t) + f_{\mathrm{tot}}(t)\Delta t \tag{7}$$

where f_{tot} includes the applied force f, the elastic forces, and the pinning forces obtained from the potential in (2). The time step Δt is chosen to be the largest possible value for which the result is independent of Δt.

3. Results

This section is divided into two parts. First we consider the quasi-static motion of the string precisely at threshold, as described in the previous section. We consider discontinuities in the energy of the string occurring when elastic energy is relased abruptly as the string jumps from one metastable state to another. These jumps can be considered as the *avalanches* of the present system [20]. We also study different measures of the roughness of the string. Next we study the motion of the string for $f - f_c$ larger than zero. We look at the velocity–force characteristic. Finally we report results on the dependence of the roughness of the string on the excess driving force $f - f_c$.

† To be precise: when $f > -f_p(h_m)$, see figure 2, for the value of $f_p(h_m)$ relevant to the actual realization of the random potential.

3.1. At threshold

In order to illustrate how the energy becomes a discontinuous function of the position of the string we will consider the interaction of the string with one single pinning centre. Figure 3 shows the variation of the string configuration and corresponding potential energy as the COM of the string is moved quasi-statically over one pinning centre. The total force on the string is always zero. Metastable states develop leading to an abrupt decrease in the energy when the string jumps onto the pinning centre and again as it jumps off [19, 12, 22, 23].

We will now consider the successive pinning and depinning of sections of the string as it is moved through a finite density of pinning centres. Figure 4 shows an example of the instantaneous configuration of a subsection of the string. This blow-up shows how the string wanders smoothly through the pinning potential. In figure 5 we plot the string configuration at successive times in the asymptotic regime where the roughness of the string has saturated (see below). One notices that the motion occurs in the form of sections which jumps ahead while other sections of the string remain statically pinned. In the late stage the string remains static for most of the time. A picture depicted by Parisi [5].

The energy of the string is suddenly decreased when the string jump from one metastable

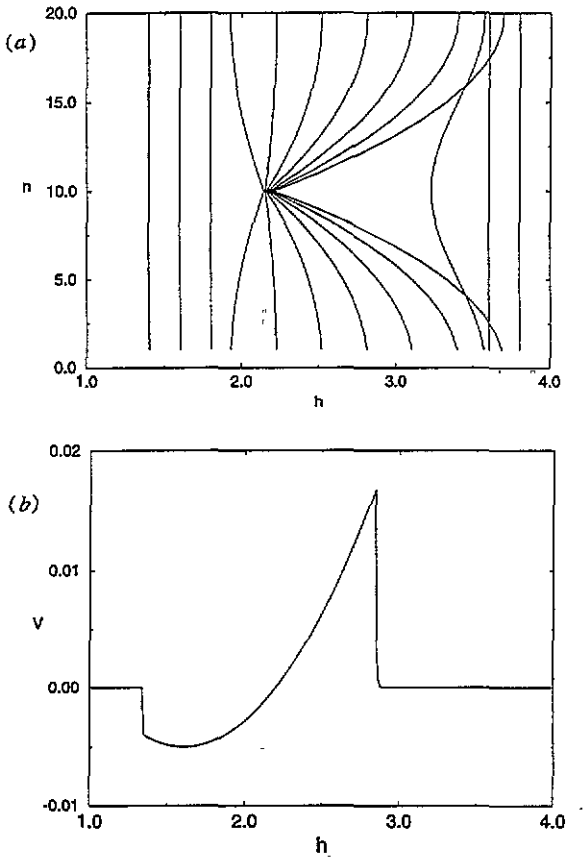

Figure 3. (*a*) Successive configurations of the string as an elastic instability is encountered. A string of length 20 is moved through a single pinning centre of strength $A_p = 0.1$, range $R_p = 0.125$, positioned at $h = 2.2$ and $n = 10$. (*b*) exhibit the discontinuous variation in the potential energy of the system during the instability.

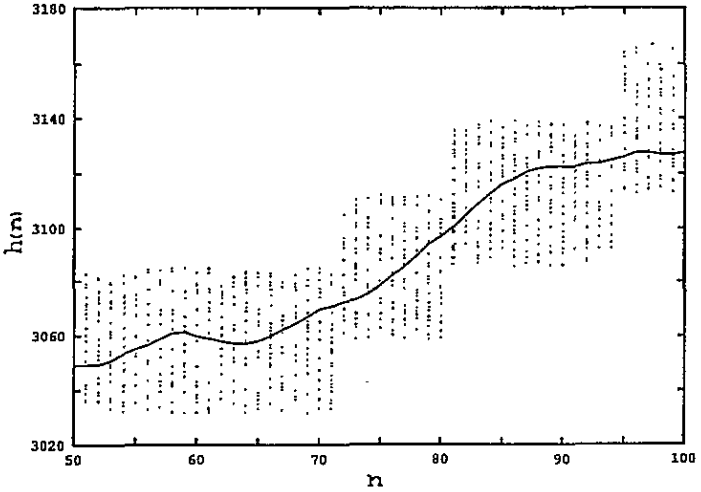

Figure 4. A subsection of an elastic string of length 640 smoothly wandering through the set of randomly positioned pinning centres all of strength $A_p = 0.5$ and range $R_p = 0.125$. The density of pinning centres is $n_p = 0.37$ along each rail.

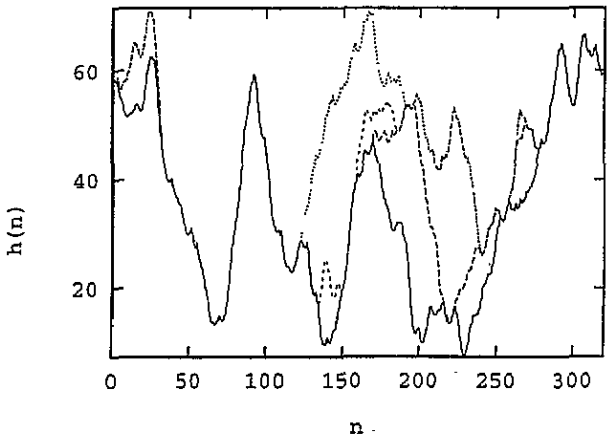

Figure 5. Plot of the string configuration at successive time instants in the saturated regime. The full curve corresponds to 6.6×10^4 time steps, the long broken curve to 7.4×10^4, the broken curve to 8.2×10^4, and finally the dotted curve corresponds to 9.0×10^4 time steps. The parameters are $L = 320$, $A_p = 0.5$, $R_p = 0.125$ and $n_p = 0.37$.

configuration to the next. Figure 6 shows the distribution of energy releases, ΔE, for different system sizes. The distribution $P(\Delta E)$ falls off exponentially for large ΔE values, see figure 6(a). In the small ΔE limit the distribution exhibits power-law behaviour, $P(\Delta E) \sim \Delta E^{-b}$ with an exponent b of about 1.4. See figure 6(b).

As the system size increases the support of the distribution $P(\Delta E)$ gradually shifts to smaller ΔE values. The exponential cutt-off region vanishes while the scaling region at small ΔE values extends to even smaller energies. A similar low-energy behaviour was observed in the simulation of the longitudinal harmonic chain [21]. The average value $\langle \Delta E \rangle$

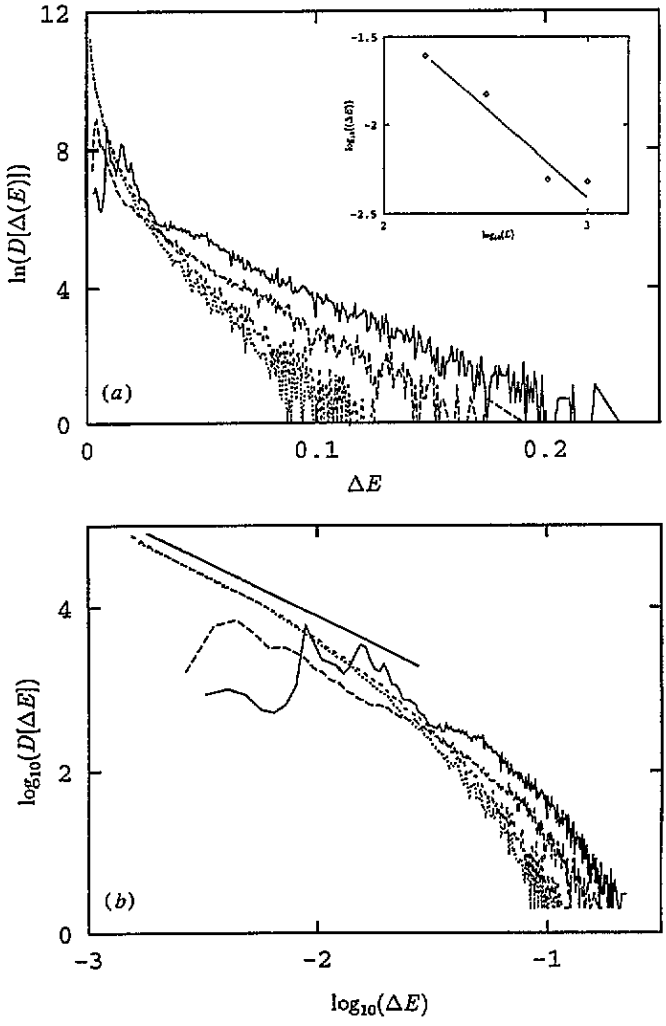

Figure 6. (*a*) Single logarithmic plot of the distribution of energy discontinuities, ΔE for different length of the chain: full curve $L = 160$, long broken curve $L = 320$, broken curve $L = 640$, and dotted curve $L = 1000$. The insert shows a double logarithmic plot of the average of ΔE for the different lengths of the chain. The straight line has slope -1. (*b*) A double logarithmic plot of the data plotted in (*a*). The straight line has slope -1.4. The parameters are $A_p = 0.5$, $R_p = 0.125$ and $n_p = 0.37$.

of ΔE scales with the length of the chain like $\langle \Delta E \rangle \sim L^{-a}$ where $a \approx 1$. See the insert in figure 6(*a*).

Below we shall (see section 5) connect the distribution of discontinuities in the energy to the average force needed to move the string through the pinning potential. This will enable us to understand the size dependens of $\langle \Delta E \rangle$. Before we finish the present section we turn to a discussion of the roughness of the string.

Roughness is most often characterized through the study of either the height correlation function or the average square width. The height correlation function is defined as

$$g(x, t) = \langle [h(x + x_0, t) - h(x_0), t]^2 \rangle_{x_0} \tag{8}$$

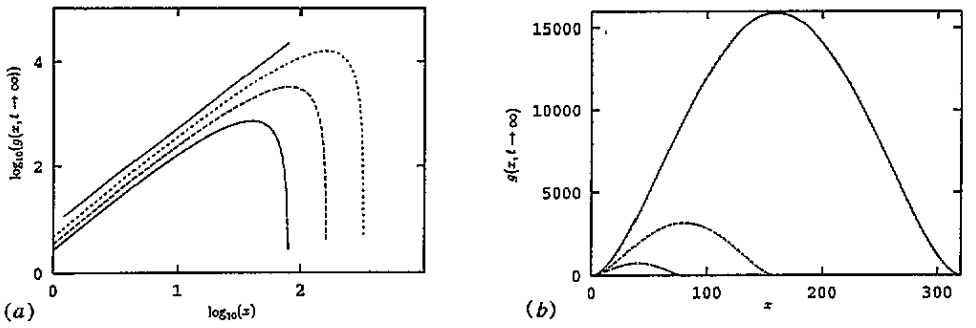

Figure 7. (*a*) Double logarithmic plot of the height correlation function defined in (8) measured in the saturated regime (averaged over time and random potential) for three different chain lengths: full curve $L = 80$, long broken curve $L = 160$, and short broken curve $L = 320$. Parameters are $A_p = 0.5$, $R_p = 0.125$, and $n_p = 0.37$. The slope of straight line is 0.9. (*b*) A linear plot of the same data as in (*a*). The figure also contains the fit to the functional form given in (9). The simulated data cannot be distinguished from the fit.

with an average (when possible) over disorder. The spatial behaviour of $g(x,t)$ is characterized by an exponent η. Namely, $g(x,t) \sim x^{2\eta}$ The measurement of η is done in the long time limit when the roughness has saturated. In figure 7(*a*) we present a double logarithmic plot of the measured $g(x) \equiv g(x, t \to \infty)$ for different system sizes. One observes an algebraic regime in which $g(x) \sim x^{2\eta}$ with $\eta \simeq 0.9$. The same value was found by Dong *et al* [6]. In the limit of large systems this exponent might, in fact, simply be equal to 1 as suggested by Narayan and Fisher [17].

The amplitude of the function $g(x)$ clearly depends on the size of the system. This suggests the following algebraic form for $g(x)$ in a periodic system:

$$g(x) = A(L)x^{2\eta}(L-x)^{2\eta} \tag{9}$$

where $A(L)$ is a size-dependent amplitude.

Figure 7(*b*) contains linear plots of the measured $g(x)$ together with fits to the form in (9). The fitted curves are obtained by putting $\eta = 0.9$ and fixing the amplitude in $x = L/2$ to the measured value. As seen from the plot one cannot distinguish the measured curve from the one obtained from (9).

Another useful measure of a surface's roughness consists in the square fluctuations in the height of the chain

$$W(t,L) = \langle [h(x,t) - \langle h(x',t)\rangle_{x'}]^2 \rangle_x . \tag{10}$$

Here the average is done over the position x over a string of a given length L. The time evolution of W during the transient period before W saturates leads to the definition of the exponent β through the expression $W(t,L) \sim t^{2\beta}$. The size dependence is subsequently studied in the limit $t \to \infty$. One defines the roughness exponent χ through $W(t \to \infty, L) \sim L^{2\chi}$.

Figure 8 contains the time and size dependence of $W(t,L)$. The simulations are started from a straight string. The early-time region during which the string moves on to the first pinning centres is characterized by a small exponent of about $\frac{1}{2}$. As soon as the string starts to move through the pinning centres this exponent changes to $\beta \approx 0.9$. This exponent is much larger than the KPZ value ($\beta_{KPZ} = \frac{1}{3}$). It is very close to the value $\beta \approx 0.95$ found for the probabilistic growth model by Sneppen [10,9] and for the slightly different model simulated by Roux and Hansen [8].

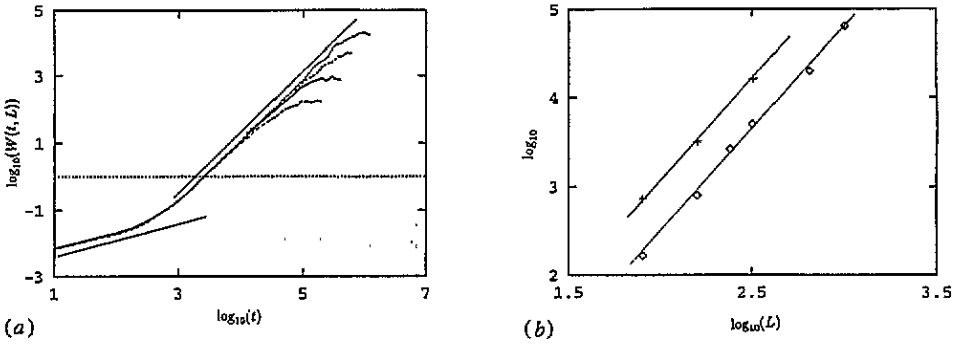

Figure 8. (*a*) Double logarithmic plot of the time dependence of $W(t, L)$ (see equation (10)) before saturation for different lengths of the chain: from bottom to top $L = 80$, 160, 320, and 640. Parameters are $A_p = 0.5$, $R_p = 0.125$ and $n_p = 0.37$. The slopes of the two straight lines are 0.5 and 1.8 respectively. (*b*) Double logarithmic plot of the dependence upon chain length of the square width $W(t \to \infty, L)$ ($\diamond$) together with the maximum amplitude $g(x = L/2, t \to \infty)$ (+) of the height correlation function. The two straight lines have the same slope, namely 2.3. The parameters are as in (*a*).

Our finding is consistent with Parisi's suggestion that systems driven precisely at the depinning transition exhibit roughening behaviour different from the KPZ values [5]. The simulated exponent β of the string is not far from experimental values for wetting in porous media. Various experiments quote different exponents from about $\beta = 0.7$–0.9 see [15].

The dependence of W upon L in the long-time limit is shown in figure 8(*b*). The roughness exponent found this way is $\chi = 1.15$, i.e. larger than one. A similar value was also observed in [7, 8]. In order to show that the behaviour of $W(t, L)$ is consistent with the measurement of $g(x, t)$ we have also plotted $g(L/2, t \to \infty)$ in figure 8(*b*). The same size scaling is observed. We conclude that the amplitude $A(L)$ of $g(x)$ (see equation (9)) scales like

$$A(L) \sim L^{2(\chi - 2\eta)}. \tag{11}$$

Thus the strain on a single chain segment is given by $g(1)^{1/2} = A(L)^{1/2}(L-1)^{\eta} \approx A(L)^{1/2}L^{\eta} \sim L^{(\chi-\eta)}$. We will discuss the implications of this result for the large-system limit $L \to \infty$ below.

The roughness exponents η and χ found here for the elastic string are different from the exponents obtained from the growth algorithms considered by Sneppen [10, 9]. Hence, we have established that the time behaviour before saturation described by this growth model is equal to the time behaviour for the continuum model defined by the elastic equation of motion (equation (4)) at least in the sense that the two models have identical β exponent. On the other hand, the roughness of the interface created by the two models is different. The Sneppen model leads to $\chi < 1$ because the microscopic updating role explicitly, and in an *ad hoc* way, only allows local slopes smaller than one. This constraint will obviously influence the roughness in the saturated regime while the constraint does not limit the early time behaviour. When the slope constraint is relaxed, as Roux and Hansen do in their version of the growth model (the Robin Hood model) [8, 9], both the temporal and spatial behaviour obtained from the equation of motion (4) are reproduced by the growth algorithm.

3.2. Above threshold

In figure 9 we present the measurement of the relationship between the disorder and time average velocity $\overline{v}$ and the applied driving force f. As discussed in section 2.1 it is difficult to access the region in the vicinity just above the threshold force. We find that in the accessible region $\overline{v}$ is well approximated by the form

$$\overline{v} \sim (f - f_c)^{\theta} \tag{12}$$

with $\theta \approx 0.5$. Dong *et al* made a great effort to study the region near the depinning [6]. They found that they could not distinguish between an algebraic form as in (12) with an exponent $\theta \approx 0.25$ and a logarithmic behaviour $v \sim 1/\log(f/f_c)$.

We found in the previous section that the string became unusually rough when driven precisely at threshold. It is interesting to see how the roughness of the string develops as the depinning threshold is approached from above. In figure 10 we plot $\log(W)$ as function of $\log(f - f_c)$ for several system sizes. We find that $W \sim (f - f_c)^{-\sigma}$ with $\sigma \simeq 3$. This result suggests the following scaling form $W = (f - f_c)^{-\sigma}\Gamma(L^{2\chi}(f - f_c)^{\sigma})$. The scaling function must behave like $\Gamma(\rho) \sim 1$ as $\rho \to 0$ and $\Gamma(\rho) \sim \rho$ as $\rho \to \infty$.

The following simple argument illuminates the dependence of W on $f - f_c$. In the continuum limit our string is described by the following Hamiltonian:

$$H = \int_0^L \mathrm{d}x \left\{ \tfrac{1}{2}\kappa(\partial_x h)^2 + V(x, h(x)) - fh(x) \right\}. \tag{13}$$

Here κ is the string tension $V(x, h(x))$ is the background potential, and f the applied driving force. The equation of motion is

$$\eta \dot{h} = -\frac{\partial H}{\partial h} = \kappa \partial_x^2 h - \frac{\partial V}{\partial h} + f \tag{14}$$

where η is a viscosity coefficient. We consider the situation above threshold $f > f_c$ and introduce a co-moving reference frame moving with the centre-of-mass velocity v of the string. The string described from this reference frame is characterized by $\tilde{h} = h - vt$. The

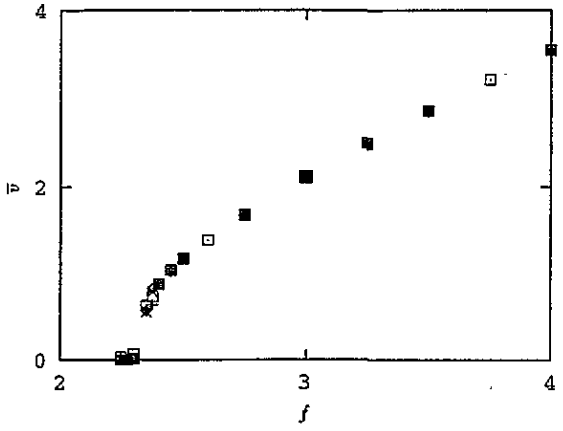

Figure 9. The time and disorder averaged centre-of-mass velocity of the chain as function applied driving force for different chain lengths: (◇) $L = 160$, (+) signs $L = 320$, (□) $L = 640$, and (×) $L = 1000$. One notice some size dependence in the vicinity of the onset of motion. Parameters are $A_p = 0.5$, $R_p = 0.125$ and $n_p = 0.37$.

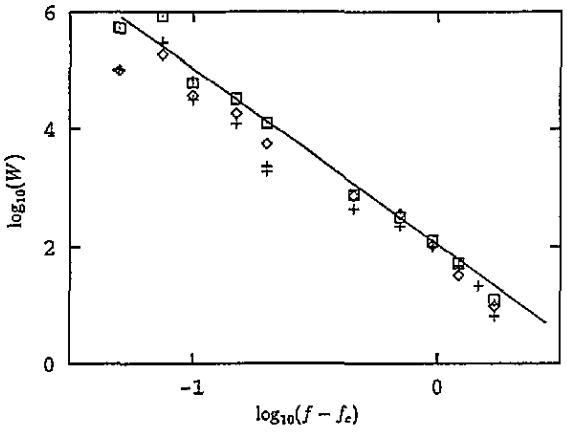

Figure 10. Double logarithmic plot of the time and disorder averaged (maximum) amplitude of the height correlation function against the difference between the applied force and the threshold force. (◇) correspond to $L = 320$, (+) to $L = 640$, and (□) to $L = 1000$. The slope of the straight line is -3. Parameters are $A_p = 0.5$, $R_p = 0.125$ and $n_p = 0.37$.

equation of motion in the co-moving frame is

$$\eta\dot{\tilde{h}} = \kappa\partial_x^2\tilde{h} + \chi(x, \tilde{h} + vt)\,. \tag{15}$$

We have lumped all forces together in one force

$$\chi(x, \tilde{h} + vt) = -\frac{\partial V(x, \tilde{h} + vt)}{\partial \tilde{h}} + f - \eta v\,. \tag{16}$$

In order to proceed we are going to replace the quenched fluctuating force term $\chi(x, \tilde{h} + vt)$ by a fluctuating term $\xi(x, t)$ which only contains annealed disorder. This is, of course, a dubious undertaking whose only virtue is to allow us to proceed. In the co-moving frame the string sees pinning centres of ranges R_p passing by at a rate $\nu = n_p v$. Imagine sitting at a fixed position x along the string. At random instances of time t_i pinning centres pass by. Let the time variation from a single pinning centre be given by $f(t)$. The fluctuating pinning force experienced at position x produced by the passage of the individual pinning centres is then given by

$$\xi(x, t) = \sum_{i=-\infty}^{\infty} f(t - t_i)\,. \tag{17}$$

The equal-position temporal correlation function is according to Campbell's theorem [23]

$$\langle\xi(x, t_1)\xi(x, t_2) = \nu\int_{-\infty}^{\infty} \mathrm{d}t f(t) f(t + |t_1 - t_2|)\,. \tag{18}$$

The function $f(t)$ will essentially have support only over a time interval given by $T = R_p/v$. Hence, it is a sensible approximation to replace the integral at the right-hand side of 18 by $T(A_p/R_p)^2\exp(-|t_1 - t_2|/T)$. The equal-time spatial correlation function can be discussed in a similar way.

Thus, it appears natural to assume the following correlator for the forces $\xi(x, T)$

$$\langle\xi(x, t)\xi(x', t')) = (n_p A_p)^2\frac{R_p}{a_0}\exp(|x - x'|/R_p)\exp(-|t - t'|/T) \tag{19}$$

with $T = R_p/v$. (Remember: n_p is the one-dimensional pinning density along the rails and a_0 denotes the spacing between the rails). The average of the square width of the string is now readily obtained from the Green's function $G(x,t)$ of (15),

$$W(\omega) \equiv \frac{1}{L}\int_o^L \mathrm{d}x\, \tilde{h}^2 = \sum_q |G(q,\omega)|^2 \langle |\xi(q,\omega)|^2 \rangle$$
$$\sim \frac{1}{\omega^2}\frac{\omega_0}{\omega^2+\omega_0^2}\sum_q \frac{1}{1+(\kappa/\eta\omega)^2 q^4}\frac{q_0}{q^2+q_0^2}. \tag{20}$$

Here $q_0 = 2\pi/R_p$ and $\omega_0 = 2\pi/T = 2\pi v/R_p$. The bombardment of the string by the pinning centres occur at a rate $\omega = 2\pi n_p v$. Thus, we consider the width when the string is driven at this frequency. The right-hand side of (20) is clearly finite as long as $\omega \sim v \sim (f - f_c)^\theta$ is non-zero. In the limit of $f \to f_c \Rightarrow v \to 0$ the expression in (20) reduces to

$$W(v) \sim v^{-4} \sim (f - f_c)^{-4\theta}. \tag{21}$$

The result of our simple discussion is that the square width of the string diverges with a power $\sigma = 4\theta$ as $f \to f_c$. We found numerically $\theta \approx \frac{1}{2}$ and would therefore expect $\sigma \approx 2$. The simulation indicates $\sigma \approx 3$. A discrepancy is not surprising given our rather cavalier treatment of the fluctuating force term.

4. Breaking of the string

In linear elasticity strain and stress are proportional, i.e. $g(1)^{1/2} \propto f_b$ where f_b denotes the total force across a spring or bond. The exponent $\chi = 1.15$ together with $\eta \leqslant 1$ implies that the extension per length of the chain $g(1)^{1/2} \sim L^{\chi-\eta}$ will grow unbounded as $L \to \infty$.

Any realistic string will break if the stress per length exceeds a certain amount. Thus the string will break when driven through the potential close to threshold.

A similar situation was found in simulations of a two-dimensional lattices in a random environment [12]. The strength of the random potential which is able to induce topological defects were found to decrease as $1/\log(L)$.

The string is torn in pieces due to the unbounded strain induced by the fluctuations in the pinning forces. Coppersmith has given an illuminating mean-field argument which explains how f_b (and therefore also $g(1)$) can grow with the system size [4]. Consider a d-dimensional system driven by a driving force equal to the depinning value $f = f_c$. Consider a region V of the system of linear extension R. The total driving force on this region is $F = R^d f = R^d f_c$. The pinning force per volume felt by the system is on average equal to f_c. The pinning force, $F_p(R)$, felt by the considered region will assume some value different from $R^d f_c$ due to spatial fluctuations. Let n_p be the density of pinning centres. The fluctuation away from the average will typically be of the order

$$\delta F \equiv |F - F_p| = \left[n_p R^d \langle f_0^2 \rangle\right]^{1/2}. \tag{22}$$

Here $\langle f_0^2 \rangle$ denotes the standard variation of the individual pinning forces. Right at threshold the forces on the region V are in balance: $F = F_p + F_b$. Here F_b denotes the total force across the boundary of the region. The aim of this consideration is to show that the force *per bond* in the boundary grows with size of the region. We have

$$F_b = F - F_p = F_c - F_p = \left[n_p R^d \langle f_0^2 \rangle\right]^{1/2}. \tag{23}$$

The forces across the boundary normalized by the volume of the boundary, R^{d-1} is given by $f_b \sim R^{d/2-(d-1)}$.

This argument suggests that the stress per bond $f_b \sim g(1)^{1/2}$ in one dimension grows as L^α with an exponent $\alpha = \frac{1}{2}$ to be compared with $\alpha \approx 0.25$ observed in the simulation. In two dimensions one expects logarithmic growth in agreement with the simulation result quoted above [12].

When linear elasticity breaks down, which is bound to happen for real springs since the extension grows unbounded, the linear connection between stress and strain is lost and the Coppersmith argument can no longer be thought of as an explanation of $\chi > 1$. The argument still, of course, predicts that the string will break since the stress increases with a positive power of the system size.

5. Pinning force and instabilities

The most celebrated attempt to calculate the pinning force produced by a collection of weak pinning centres is the theory by Larkin and Ovchinnikov (LO) [11]. Here we briefly sketch the LO argument applied to our elastic chain. The pinning force is estimated from the fluctuations in the pinning forces within a correlated region of size L_c:

$$f_p = \left[n_p L_c R_p \langle f_0^2 \rangle\right]^{1/2} / L_c \,. \tag{24}$$

The size of the correlated region is obtained from the energy. The pinning potential induces an extension of the chain of order R_p over the length of the correlated region. This leads to an increase of the elastic energy of order $E_{el} = k(R_p/L_c)^2$ and a decrease in the pinning energy of the order $E_{pin} = -R_p f_p$. Minimizing $E = E_{el} + E_{pin}$ with respect to L_c determines L_c in terms of the model paramenters and f_p. Substitution into (24) leads to an expression for f_p which behaves like $f_p \sim \langle f_0^2 \rangle^{2/3}$. In our case we will have $\langle f_0^2 \rangle \sim (A_p/R_p)^2$†. Accordingly the LO theory predicts that f_p scales like $A_p^{4/3}$.

In figure 11 we show a double logarithmic plot of the depinning force f_c estimated

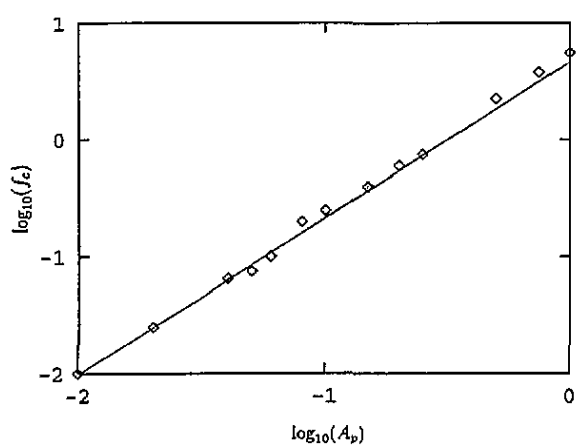

Figure 11. Double logarithmic plot of the threshold force against the amplitude of the pinning centres. The slope of the straight line is equal to $\frac{4}{3}$ in accordance with collective pinning theory. Parameters are $L = 320$, $R_p = 0.125$ and $n_p = 0.37$.

† It should be noted that the LO theory assumes the pinning forces to be uncorrelated with the elastic medium when $\langle f_0^2 \rangle$ is estimated.

from the velocity–force curves as a function of A_p. We find that $f_c \sim A_p^n$ with $n = \frac{4}{3}$ as is seen from the agreement between the straight line (of slope $\frac{4}{3}$) and the data points of the simulation. Hence, the depinning force appears to be well estimated by the LO argument. We did not encounter the same agreement previously in two dimensions [12]. The deviation between the data points and the straight line observed in the region near $A_p = 1$ is to be expected. This occurs when $L_c \approx 1$.

The LO estimate of f_p as presented above is a static scaling force. It makes no reference to the elastic instabilities responsible for the existence of a non-zero threshold force [26, 19, 12, 22, 23]. For this reason the agreement shown in figure 11 between scaling of the LO expression and the simulated depinning force is remarkable.

In order to make a connection to the elastic instabilities we will consider another measure of the threshold force. Namely, the average pinning force, $\bar{F}$, experienced during a quasi-static shift at the depinning threshold (see section 2.1 above). We define [13, 26]

$$\bar{F} = \lim_{L\to\infty} \frac{1}{L} \int_0^L f_p(h)\, dh \tag{25}$$

where $f_p(h)$ denotes the pinning force (for a given realization of the pinning potential) acting on the string at the centre-of-mass position h. In the limit of vanishing velocity of the string $\bar{F}$ is a good measure of the depinning force. Moreover, we will now show how $\bar{F}$ is connected to the distribution of energy discontinuities. This will enable us to understand the observed size scaling of the average energy release $\langle \Delta \rangle$.

Whenever the total energy of the string is a smooth function of the string position h one finds that [13, 26]

$$f_p(h) = \partial U / \partial h\,. \tag{26}$$

This expression allows us to establish a convenient connection between $\bar{F}$ and the discontinuities in the total energy of the string. See figure 3. Substituting (26) into (25) we obtain (h_d denotes the positions where the discontinuity occur)

$$\begin{aligned} \bar{F} &= \lim_{L\to\infty} \sum_{h_d} \Delta E(h_d) \\ &= \nu \int \Delta E P(\Delta E)\, d(\Delta E) \\ &= \nu \langle \Delta E \rangle\,. \end{aligned} \tag{27}$$

Here ν denotes the number of discontinuities encountered per unit shift of the string. In our case, where the string is defined by a fixed number of beads and the pinning centres all sit on the rails, (see figure 1) we have $\nu \propto 1/L$. Thus, if we assume that $\lim_{L\to\infty} \bar{F} \to$ constant $< \infty$† we must have $\langle \Delta E \rangle \sim 1/L$. This was in fact the scaling observed in the insert of figure 6(*a*).

6. Summary and discussion

We have studied an elastic string in a random potential. The continuous string is replaced by a set of beads elastically coupled together. The position of the beads are continuum variables restricted to straight rails. We find that the strain *per length* of the chain induced by the random potential growth with the chain length as the string is moved through the

† The work (per chain length) needed to enter the steady state in which $W(L, t)$ has saturated might diverge with L since $g(1)$ diverges with L. This does not imply that the work (again per chain length) needed to maintain the saturated state diverges with L.

random background at the depinning threshold. The roughness of the string is characterized by three scaling exponents $\beta \simeq 0.9$, $\eta \simeq 0.9$ and $\chi \simeq 1.15$. The exponent β describes the early temporal evolution of the roughness as the string is started out form the straight configuration. The exponent η describes spatial dependence of the height correlation function $g(x) = A(L)x^{2\eta}(L-x)^{2\eta}$ in the regime where the roughness has saturated. The exponent χ controls the size dependence of the amplitude $A(L) \sim L^{2(\chi-2\eta)}$.

Our model does not contain a threshold condition in the definition of the microscopic update of the model. Abrupt depinning events with sudden releases of bursts of energy occur as a consequence of elastic instabilities. The distribution of energy releases *per length* exhibit algebraic behaviour in the region of small energies followed by an exponential tail in the high-energy regime. We find that the average energy release decreases as one over the length of the chain. This was explained by making a connection between the average energy release and the average force needed to move the string through the background potential.

We have compared our simulation of the dynamics derived from the equation of motion for an elastic chain with various growth algorithms. Overall we find agreement between our simulation of the equation of motion and the simulations of cellular automata or coupled lattice-map-like models. There is, though, one important exception. The growth model studied by Sneppen [8–10] has $\chi < 1$ instead of $\chi > 1$ as found for the elastic chain. The reason is that Sneppen's update algorithm constricts the local slope.

Since $\chi > 1$ the elastic string will inevitably break as the length of the string is increased. This implies that there exists no weak-pinning elastic limit of the depinning transition. This is also the case in higher dimensions [12, 4]. A realistic study of interface growth and depinning must allow for breaking of the interface. Precisely how the breaking takes place will depend on the specific system considered. A liquid interface will close in behind obstacles, a flux line in a superconductor will leave small flux loops behind at regions of stronger pinning. The breaching of the interface will decrease the fluctuations in the width of the interface. As a consequence we expect χ to decrease. The actual value of χ will probably depend on the relevant mechanism by which the interface breaks. Hence, for systems of a size large enough to make the elastic description insufficient we do not expect the existence of a single universal exponent χ.

Acknowledgments

I appreciate stimulating discussions with M H Jensen, K Sneppen, L-H Tang, G Blatter, V B Geshkenbein, and A Larkin. This work is supported by the British EPSRC.

References

[1] di Meglio J-M 1992 *Europhys. Lett.* **17** 607
[2] Andersen J Vitting and Brechet Y 1994 *Phys. Rev. Lett.* **73** 2087
[3] Blatter G, Feigel'man M V, Geshkenbein V B, Larkin A I and Vinokur V M 1995 *Rev. Mod. Phys.* at press
[4] Coppersmith S N 1990 *Phase Transitions and Relaxation in Systems with Competing Energy Scales* ed T Riste and D Sherrington (Dortrecht: Kluwer); 1990 *Phys. Rev. Lett.* **65** 1044
[5] Parisi G 1992 *Europhys. Lett.* **17** 673
[6] Dong M, Marchetti M C, Middleton A A and Vinokur V 1993 *Phys. Rev. Lett.* **70** 662
[7] Leschhorn H and Tang L-H 1993 *Phys. Rev. Lett.* **70** 2973
[8] Roux S and Hansen A 1994 *J. Physique I* **4** 515
[9] Zaitsev S I 1992 *Physica* **189A** 411
[10] Sneppen K 1992 *Phys. Rev. Lett.* **69** 3539
Tang L-H and Leschhorn H 1993 *Phys. Rev. Lett.* **70** 3832
Olami Z, Procaccia I and Zeitak R 1994 *Phys. Rev.* E **49** 1232

Leschhorn H and Tang L-H 1994 *Phys. Rev.* E **49** 1238
[11] Larkin A I and Ovchinnikov Yu N 1979 *J. Low Temp. Phys.* **34** 409
[12] Jensen H J, Brass A and Berlinsky A J 1988 *Phys. Rev. Lett.* **60** 1676
Brass A, Jensen H J and Berlinsky A J 1989 *Phys. Rev.* B **39** 102
[13] Jensen H J, Brechet Y and Brass A 1989 *J. Low Temp. Phys.* **74** 293
[14] Kardar M, Parisi G and Zhang Y C 1986 *Phys. Rev. Lett.* **56** 889
[15] See, for example, Vicsek T, Cserzo M and Horvath H K 1990 *Physica* **167A** 315
Rubio M A, Edwards C A, Dougherty A and Gollub J P 1989 *Phys. Rev. Lett.* **63** 1685
Horvath V K, Family F and Vicsek T 1990 *Phys. Rev. Lett.* **65** 1388; 1991 *Phys. Rev. Lett.* **67** 3207
[16] Nattermann T, Stepanow S and Tang L-H 1992 *J. Physique II* **2** 1483
[17] Narayan O and Fisher D S 1993 *Phys. Rev.* B **48** 7030
[18] Kessler D A, Levine H and Tu Y 1991 *Phys. Rev.* A **43** 4551
[19] Brandt E H 1983 *J. Low Temp. Phys.* **53** 41, 71
[20] Bak P, Tang C and Weisenfeld K 1987 *Phys. Rev. Lett.* **59** 381
[21] Jensen H J, Brechet Y and Doucot B 1993 *J. Physique I* **3** 611
[22] Jensen H J, Brechet Y, Doucot B and Brass A 1993 *Europhys. Lett.* **23** 623
[23] MacDonald D K C 1962 *Noise and Fluctuations: an Introduction* (New York: Wiley)
[24] Jensen H J *Phase Transitions and Relaxation in Systems with Competing Energy Scales* ed T Riste and D Sherrington (Dortrecht: Kluwer)